

# High-Temperature Superconducting Coil Option for the LHD-Type Fusion Energy Reactor FFHR

Gourab BANSAL, Nagato YANAGI<sup>1</sup>), Tsutomu HEMMI<sup>2</sup>), Kazuya TAKAHATA<sup>1</sup>), Toshiyuki MITO<sup>1</sup>) and Akio SAGARA<sup>1</sup>)

*The Graduate University for Advanced Studies, Toki, Gifu 509-5292, Japan*

<sup>1</sup>*National Institute for Fusion Science, Toki, Gifu 509-5292, Japan*

<sup>2</sup>*Japan Atomic Energy Agency, 801-1, Mukoyama, Naka 311-0193, Japan*

(Received 17 November 2007 / Accepted 23 February 2008)

Large-current-capacity high-temperature superconducting (HTS) conductors using YBCO tapes are being considered as an option for the LHD-type fusion energy reactor FFHR. The typical operating current, magnetic field, and temperature of such conductors in FFHR are 100 kA, 13 T, and 20 K, respectively. A preliminary design of the HTS conductor has been proposed for the FFHR helical coils. Analyses have been performed on the proposed HTS conductor regarding thermal properties, mechanical structures, AC losses, and quench detection and protection. It is suggested that stainless steel might be a better choice for the outer jacket of the HTS conductor compared to aluminum alloy. Due to increased specific heats of conductor materials at 20 K, HTS magnets are supposed to be operated more stably compared to low-temperature superconducting (LTS) magnets operated at  $\sim 4$  K. The required refrigeration power is also reduced. Therefore, using HTS conductors, it is considered to be viable to assemble the continuous helical coils in segments with joints of conductors, as additional heat generation at the joints can be taken care by utilizing the surplus refrigeration power. According to these analyses, HTS conductors seem to be promising for the FFHR coils.

© 2008 The Japan Society of Plasma Science and Nuclear Fusion Research

Keywords: LHD, FFHR, fusion reactor, HTS, YBCO, BSCCO, superconductor, stability

DOI: 10.1585/pfr.3.S1049

## 1. Introduction

The LHD-type fusion energy reactor, FFHR, is being designed at the National Institute for Fusion Science (NIFS) in the framework of inter-university collaborative researches [1]. Several design options of FFHR have been proposed [2] and among them, the recent design FFHR-2m1 has a plasma major radius of 14 m, toroidal field of 6.18 T, maximum field at the conductor of 13 T, and fusion power of 1.9 GW. FFHR-2m1 consists of a pair of helical coils and two pairs of poloidal field coils. In the present design, well-developed low-temperature superconductors (LTS) are being considered for application in the coils. However, recently, high-temperature superconducting (HTS) technology has improved significantly and has shown good prospects for future applications [3–7]. Considering this fact, HTS has emerged as a competitive candidate for FFHR [8].

In particular, high-temperature superconductors are being considered for high-field magnets in fusion reactors due to their better performance in a strong magnetic field with elevated temperature operation [9–13]. When HTS magnets are operated in fusion reactors at a temperature of  $\sim 20$  K or higher, the operational cost can be reduced compared to conventional LTS magnets, which

need to be operated only at  $\sim 4$  K. Second, due to the increased specific heat of HTS conductors at elevated temperatures, they become less prone to quenching, and therefore, safer operation of fusion reactors is possible, which is the most desirable requirement for the magnets. Moreover, the increased thermal conductivities of metals at elevated temperatures and larger allowable temperature gradient help in quickly removing the heat generated in the conductor due to AC losses, mechanical disturbances, nuclear heating, and other sources. HTS magnets can be cooled by conduction cooling methods and can avoid having complicated piping networks, generally necessary for forced-flow-cooled LTS magnets. Even though there still are many issues to be solved before large-current-capacity HTS conductors are viable, the above advantages are worth being considered to overcome the difficulties in developing such conductors. One of the most difficult issues is found in the mechanical strength of conductors since HTS materials are basically brittle ceramics.

The present study is focused on the HTS conductor design for the helical coils of FFHR. Here, an indirect cooling method proposed for the aluminum-alloy jacketed Nb<sub>3</sub>Sn conductor [14] is also adopted for HTS conductors. In the present work, analyses have been performed on the proposed HTS conductor regarding thermal

author's e-mail: bansal@nifs.ac.jp

properties, mechanical structures, AC losses, and quench detection and protection. Segmented helical coils are considered to be viable for FFHR due to the advantages of HTS conductors.

## 2. HTS Conductor Design

The second-generation HTS conductors, such as YBCO and GdBCO coated-conductors, may become promising candidates for future demo fusion reactors, since they sustain high critical currents at high magnetic fields. A cross-sectional view of the proposed 100 kA-class HTS conductor for the FFHR coils is shown in Fig. 1. This conductor uses stacks of YBCO tapes along with additional copper tapes inside a thick jacket of aluminum alloy (6061-T6) or stainless steel. The size of the conductor has been chosen same as that for the LTS counterpart proposed in [14]. The critical current of the HTS tape is set as 100 A/mm-width at 13 T and 25 K, which is expected to be available in the near future. The copper to superconductor ratio in HTS conductor is 7.0 and the critical current of the conductor is 128 kA at 13 T, 25 K.

We consider that there are remarkable advantages with a simple stacked-type configuration, such as (a) cabling technique is simple, (b) no degradation of HTS tapes occurs due to bending or twisting, and (c) there is no cross-over point, which is supposed to be mechanically weak. Even though non-uniform current distribution might be formed with such a configuration due to the inductance mismatching between tapes, its effects on cryogenic stability is considered to be small due to the high intrinsic stability of HTS at elevated temperatures.

Figure 2 shows a cross-sectional image of the helical coil (1.8 m wide and 0.9 m thick). The helical coil consists of 12 layers with 36 turns in each layer. Inside the winding, there are four 75-mm-thick cooling panels with embedded cooling channels where the coolant flows. The windings

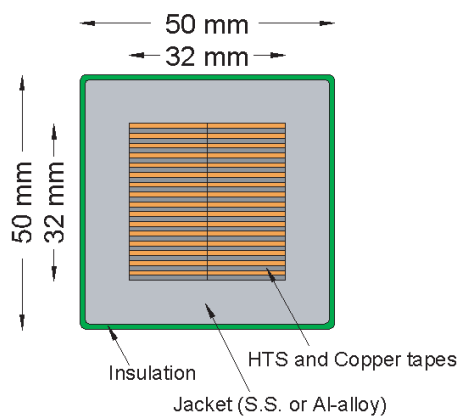


Fig. 1 Cross-sectional view of the proposed HTS conductor for the FFHR coils. Here, “S.S.” and “Al-alloy” stand for stainless steel and aluminum alloy (6061-T6), respectively.

are cooled by thermal conduction from the cooling panels. The expected steady-state nuclear heat load on the superconducting coils in FFHR is about 100 W/m<sup>3</sup> [14, 15], which should be removed by the coolant effectively. The temperature increase of the conductor,  $\Delta T_{\max}$ , can be estimated by a one-dimensional heat conduction equation,

$$\Delta T_{\max} = \frac{Ql^2}{2\lambda_e}, \tag{1}$$

where  $Q$  is the heat load,  $l$  is the distance, and  $\lambda_e$  is the effective thermal conductivity.

In Fig. 2, the maximum distance between the heated zone and coolant,  $l$ , is assumed to be 0.1 m. If the conductor temperature is allowed to be increased by 1 K for nuclear heating of 100 W/m<sup>3</sup>, the required effective thermal conductivity is 0.5 W/m-K.

Figure 3 shows the calculated effective thermal conductivity over a length of 0.1 m in the winding cross-section. The insulation thickness is taken as 1 mm and its thermal conductivity is 0.1 W/m-K at 20 K. The effective thermal conductivity is calculated by varying the thermal conductivities of the jacket as well as the HTS and

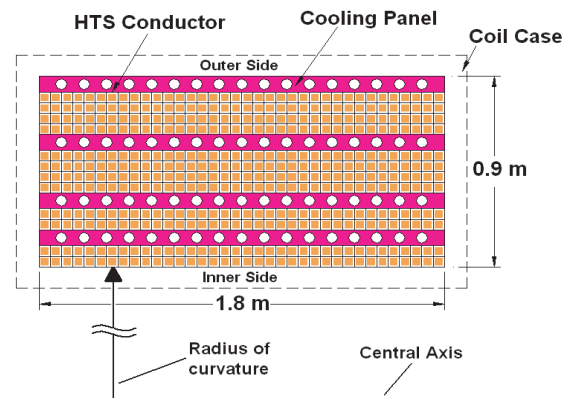


Fig. 2 Cross-sectional view of the helical coil of FFHR.

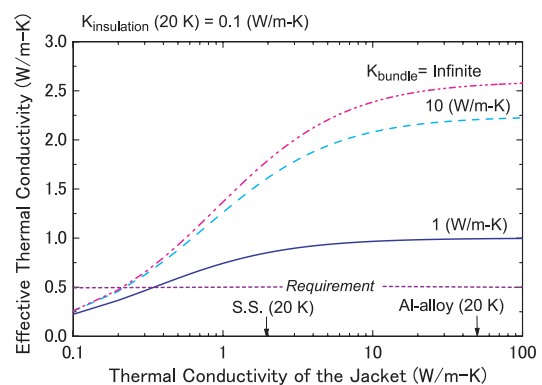


Fig. 3 Effective thermal conductivity in the cross-sectional direction of the windings as a function of the thermal conductivities of the jacket and HTS bundle. Here, “S.S.” and “Al-alloy” stand for stainless steel and aluminum alloy (6061-T6), respectively.

copper tape bundles. In the worst case, when the thermal conductivity of the HTS and copper tape bundles is assumed to be  $1 \text{ W/m-K}$  and the conductor jacket is of stainless steel, the effective thermal conductivity is calculated to be  $\sim 0.85 \text{ W/m-K}$  at  $20 \text{ K}$ . This value is still higher than the required effective thermal conductivity of  $0.5 \text{ W/m-K}$ , suggesting that stainless steel can also be used in HTS conductors, which is not possible for the LTS counterpart proposed in [14]. An Aluminum-alloy jacket provides a higher effective thermal conductivity of  $\sim 1 \text{ W/m-K}$  at  $20 \text{ K}$ , and therefore, is a better option as far as heat removal is concerned.

### 3. Stress and Strain in the Helical Coils

The helical coils of FFHR will experience large electromagnetic forces, and therefore, the stress and strain will be developed in the coils. Here, the stress and strain are estimated by considering the coil as an infinite solenoid, and only the radial forces are taken into account [14, 16]. The average radius of curvature of the helical coil is  $5.5 \text{ m}$ , and therefore, the same radius of curvature is considered for an infinite solenoid model. The cross-sectional area of the solenoid model is also the same as that of the helical coil shown in Fig. 2.

The calculated stress and strain, using analytic solutions for an infinite solenoid model, are shown in Fig. 4 for the two cases with an aluminum alloy jacket and stainless steel jacket. For the conductor cross-section, the effective Young's modulus is calculated using the mixture

rule considering hardened copper tapes and YBCO tapes with Hastelloy substrates inside either an aluminum alloy or stainless steel jacket and GFRP insulation over the HTS conductor. The Young's moduli of copper, HTS tapes, aluminum alloy, stainless steel, and GFRP insulation at  $20 \text{ K}$  are considered to be  $140, 200, 80, 200,$  and  $20 \text{ GPa}$ , respectively. The effective Young's moduli for an HTS conductor cross-section are calculated to be  $101$  and  $167 \text{ GPa}$  for aluminum-alloy and stainless-steel jacketed conductors, respectively.

Zero radial stresses at the inner and outer radius of the windings are taken as the boundary conditions. The maximum hoop stress in the stainless-steel cooling panel and the aluminum-alloy jacketed HTS conductor are  $470$  and  $250 \text{ MPa}$ , respectively. The maximum hoop stress in the conductor is  $335 \text{ MPa}$  when the HTS conductor jacket is of stainless steel. The stress is always less than the yield strength of the materials at  $20 \text{ K}$  ( $380 \text{ MPa}$  for aluminum-alloy and  $1050 \text{ MPa}$  for stainless steel), and therefore, the coil is supposed to be safe under large electromagnetic forces in FFHR. The hoop strain is less than  $0.2\%$  for the case with the stainless-steel jacket. The bending strain is about  $0.32\%$  in FFHR with the present design of the HTS conductor, as shown in Fig. 1, and therefore, the total strain would be about  $0.5\%$ . The critical strain for YBCO is about  $0.7\%$ , above which the critical current starts to degrade [17]. For reducing the bending strain in the conductor, a rectangular-shaped HTS conductor design is also being considered, which will be reported elsewhere.

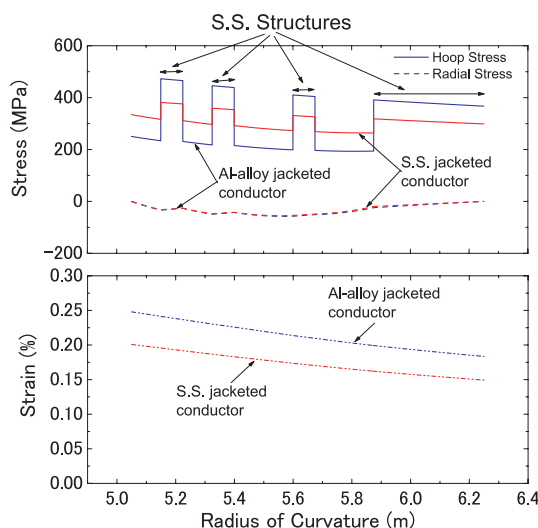


Fig. 4 Calculated stress and strain in the FFHR helical coils. Here, “S.S.” and “Al-alloy” stand for stainless steel and aluminum alloy (6061-T6), respectively. The “Al-alloy jacketed conductor” means that the conductor jacket is made of aluminum alloy but cooling panels are made of stainless-steel, whereas the “S.S. jacketed conductor” means that both the conductor jacket and the cooling panels are made of stainless steel.

### 4. Quench Detection and Protection

Due to the increased specific heat of the materials at elevated temperatures, the thermal diffusivity becomes smaller and therefore the quench propagation also becomes slower. Hence, the voltage development in HTS conductors at elevated temperatures is very slow and therefore the quench detection becomes more difficult than when using LTS conductors. This is one of the concerns in HTS conductors.

During a normal transition, the current redistribution from one HTS tape to another is important to avoid overheating of HTS tapes. The expected contact resistance between two soldered YBCO tapes, having a resistive substrate and buffer layers between two YBCO layers, is about  $0.02 \mu\Omega$  for a  $1 \text{ m}$  overlap length, which is of the same order or smaller than that in cable-in-conduit conductors having non-insulated strands. Since current redistribution is not a serious problem in cable-in-conduit conductors with non-insulated strands [18], the current redistribution between HTS tapes in the proposed HTS conductor might not be a serious problem. Furthermore, there has been some progress toward the development of copper substrate-based YBCO tapes with conductive buffer layers [19]. Using such YBCO tapes, the current transfer from one YBCO tape to others will no longer remain an issue.

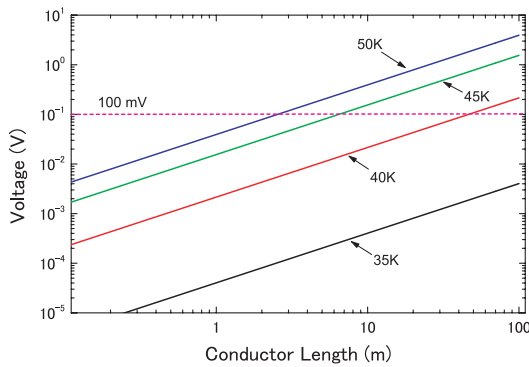


Fig. 5 Voltage development as a function of conductor length at different temperatures with 100 kA current.

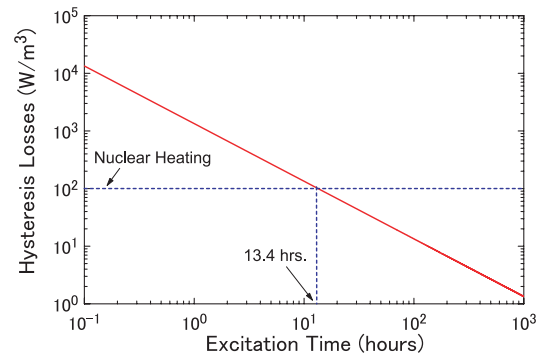


Fig. 7 Hysteresis losses as a function of excitation time up to the peak field of 13 T in the FFHR helical coils.

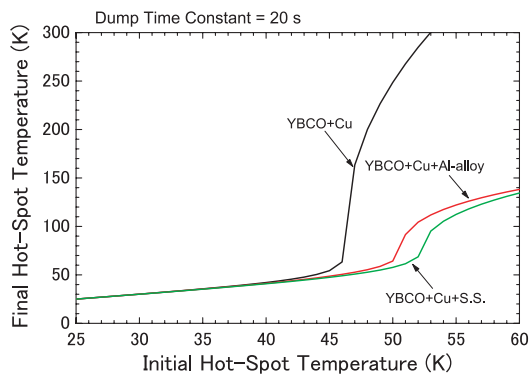


Fig. 6 Final hot-spot temperature as a function of the initial hot-spot temperature (just before dumping) for different jacket materials. Here, “Cu,” “S.S.,” and “Al-alloy” stand for copper, stainless steel, and aluminum alloy (6061-T6), respectively.

Figure 5 shows the expected voltage along the conductor as a function of the conductor length at different temperatures with 100 kA current. At 45 K, the conductor length is about 6 m to observe a voltage of 100 mV for quench detection, whereas it is about 2.5 m at 50 K. The required length further reduces with increased temperature. Thus, higher the allowable initial hot-spot temperature, easier it is to detect a quench.

Figure 6 shows the final hot-spot temperature with different jacket materials in the adiabatic condition as a function of the initial temperature of a hot-spot. The coil current is 100 kA at the operating temperature of 25 K, and the stored magnetic energy is dumped into an external resistor with a time constant of 20 s after quench detection. Figure 6 suggests that the stainless-steel jacket for the HTS conductor allows higher initial hot-spot temperature before discharging (for the condition that gives the final hot-spot temperature below 150 K). This means that a shorter conductor length is required to develop larger voltage, as shown in Fig. 5, and therefore, a quench can be detected quickly and easily with a stainless-steel jacketed HTS conductor.

## 5. AC Losses and Coil Excitation Time

The AC losses during excitations are always a concern for any superconducting magnet. The ramp-up rate should be chosen in such a way that the temperature rise of the magnet is acceptable by the cooling of coil windings. The smaller losses are required to reduce the overall refrigeration power as well. The hysteresis losses are the dominant contributions in HTS conductor magnets. Figure 7 shows the expected hysteresis losses per unit volume of the windings as a function of excitation time up to the peak field of 13 T at the innermost conductors in the FFHR helical coils. As shown in Fig. 7, in order to suppress hysteresis losses equivalent to the steady-state nuclear heating of 100 W/m<sup>3</sup>, the excitation time should be about 13 hours.

## 6. Proposal of Segmented Helical Coils

It may not be easy to realize a continuous winding of the huge helical coils in FFHR; therefore, segmented helical coils might be a viable choice to wind the helical coils with a number of joints between segments [20]. Due to the elevated temperature operation of HTS coils, the surplus refrigeration power can be used to take away the heat generated by the joints between segments. Since an HTS conductor has a large temperature margin, the temperature rise of a few Kelvin due to the joints may not be a big concern for the stability of the coils.

Figure 8 shows the expected maximum temperature rise of the conductor as a function of heating density calculated by Eq. (1). Both the options for the conductor jacket, stainless steel and aluminum alloy, are considered. For a temperature rise of 5 K in the conductor, a heating density of about 990 W/m<sup>3</sup> on the windings can be allowed. This means that a joint resistance of about 3 nΩ is acceptable. The joint between the conductors might be a mechanical joint [20] or a simple soldered lap joint. Here, we propose a conceptual illustration of a soldered joint configuration, as shown in Fig. 9. The HTS tapes are cut in step-like structures and then overlapped and joined with YBCO sides facing each other.

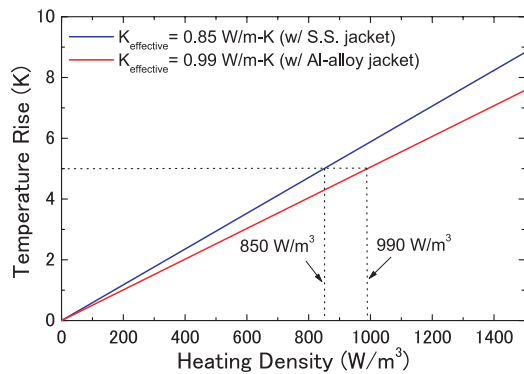


Fig. 8 Maximum temperature rise of the conductor as a function of the heating density on the helical coil windings. Here, “S.S.” and “Al-alloy” stand for stainless steel and aluminum alloy (6061-T6), respectively.

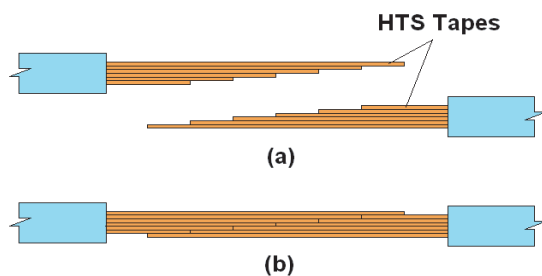


Fig. 9 Schematic illustration of (a) HTS tapes cut in step-like structures and (b) overlap joint between two HTS conductors.

## 7. Summary

Feasibility studies of an HTS conductor option for the LHD-type fusion energy reactor FFHR have started. A preliminary design of an indirectly cooled HTS conductor with a stack of YBCO tapes is proposed. Quench detection and stress calculations suggest that stainless steel is better as a jacket material for the conductor. On the other hand,

aluminum alloy, being a softer material, might be a better choice from the winding point of view. Segmented helical coils with soldered lap joints might be a viable choice considering the large temperature margin of the HTS conductor and available surplus refrigeration power, which is a big advantage with HTS conductors over their LTS counterparts. More studies, such as error magnetic fields generated by shielding currents, current distribution in the conductor, and AC losses are being investigated on the HTS conductors and will be reported elsewhere. Moreover, with the aim of developing a 100-kA HTS conductor, a prototype 10 kA-class HTS conductor has been developed and tested successfully [21].

- [1] A. Sagara *et al.*, Fusion Eng. Design **81**, 2703 (2006).
- [2] A. Sagara *et al.*, Nucl. Fusion **45**, 258 (2005).
- [3] J.R. Hull, Jour. Nucl. Materials **191-194**, 520 (1992).
- [4] G. Janeschitz *et al.*, Fus. Eng. Design **81**, 2661 (2006).
- [5] P. Komarek, Fus. Eng. Design **81**, 2287 (2006).
- [6] W.H. Fietz *et al.*, Fus. Eng. Design **75-79**, 105 (2005).
- [7] L. Bromberg *et al.*, Fus. Eng. Design **54**, 167 (2001).
- [8] T. Hemmi *et al.*, Annual Report of National Institute for Fusion Science, ISSN **0917-1185**, 278 (2007).
- [9] T. Ando *et al.*, presented at SOFE 2005.
- [10] F. Dahlgren *et al.*, Fus. Eng. Design **80**, 139 (2006).
- [11] T. Isono *et al.*, Fus. Eng. Design **81**, 1257 (2006).
- [12] W Goldacker *et al.*, J. Phys. Conf. Ser. **43**, 901 (2006).
- [13] T. Isono *et al.*, IEEE Trans. Appl. Supercond. **13**, 1512 (2003).
- [14] K. Takahata *et al.*, Fus. Eng. Design **82**, 1487 (2007).
- [15] A. Sagara *et al.*, Fus. Eng. Design **81**, 1299 (2006).
- [16] M.N. Wilson, *Superconducting Magnets*, (Clarendon Press, Oxford, 1983) p. 41.
- [17] K. Shikimachi *et al.*, Journal of Physics: Conference Series **43**, 547 (2006).
- [18] G. Bansal *et al.*, to be published in IEEE Trans. Appl. Supercond., June (2008).
- [19] K. Kim *et al.*, Supercond. Sci. Technol. **19**, R23 (2006).
- [20] H. Hashizume *et al.*, J. Plasma Fusion Res. SERIES **5**, 532 (2001).
- [21] G. Bansal *et al.*, to be published in IEEE Trans. Appl. Supercond., June (2008).